Anal. Chem. **2010,** *82,* 9941–9947

Automated Microfluidic Screening Assay Platform Based on DropLab

Wen-Bin Du,† Meng Sun, Shu-Qing Gu, Ying Zhu, and Qun Fang*

Institute of Microanalytical Systems, Department of Chemistry, Zhejiang University, Hangzhou 310058, China

This paper describes DropLab, an automated microfluidic platform for programming droplet-based reactions and screening in the nanoliter range. DropLab can meter liquids with picoliter-scale precision, mix multiple components sequentially to assemble composite droplets, and perform screening reactions and assays in linear or two-dimensional droplet array with extremely low sample and reagent consumptions. A novel droplet generation approach based on the droplet assembling strategy was developed to produce multicomponent droplets in the nanoliter to picoliter range with high controllability on the size and composition of each droplet. The DropLab system was built using a short capillary with a tapered tip, a syringe pump with picoliter precision, and an automated liquid presenting system. The tapered capillary was used for precise liquid metering and mixing, droplet assembling, and droplet array storage. Two different liquid presenting systems were developed based on the slotted-vial array design and multiwell plate design to automatically present various samples, reagents, and oil to the capillary. Using the tapered-tip capillary and the picoliter-scale precision syringe pump, the minimum unit of the droplet volume in the present system reached ~20 pL. Without the need of complex microchannel networks, various droplets with different size (20 pL−25 nL), composition, and sequence were automatically assembled, aiming to multiple screening targets by simply adjusting the types, volumes, and mixing ratios of aspirated liquids on demand. The utility of DropLab was demonstrated in enzyme inhibition assays, protein crystallization screening, and identification of trace reducible carbohydrates.

In recent years, droplet-based microfluidics has attracted great interest due to its abilities of eliminating dispersion,[1−4] accelerating mixing,[1,2] providing control over the chemical and physical environment,[3,4] and having great potential in high-throughput screening.[1,4] Various microfluidic techniques for droplet mixing,[5] fission and fusion,[6] sorting,[6,7] and detection[8] have been well developed. Many systems have been successfully applied in protein crystallization,[9] single cell analysis,[10] nucleic acid-based assays,[11] enzyme kinetics studies,[12] and chemical synthesis.[13]

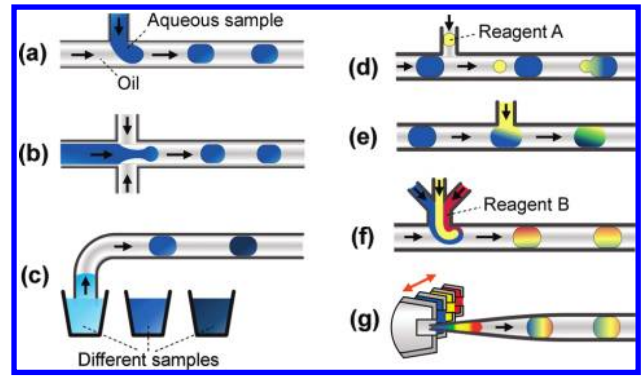

Figure 1. Various droplet generation modes used in droplet-based microfluidic systems based on T-junction (a), flow-focusing (b), and cartridge (c) techniques. Various reagent mixing modes for droplets based on droplet fusion (d), postmixing (e), and premixing (f) techniques. (g) Droplet assembling mode combining droplet generation with reagent mixing.

Liquid handling in routine laboratories usually requires metering and mixing of samples and reagents for reactions and assays. Many experiments also need to screen multiple samples or reagents and different mixing ratio conditions. Among the reported droplet-based systems, T-junction[14] and flow-focusing[15] techniques (as shown in Figure 1a,b) are frequently adopted to continuously generate droplets utilizing the oil−aqueous interface instability. Reagents are usually mixed with samples before (Figure 1f) or after (Figure 1d,e) droplet generation.[1] As in other microfluidic devices, the throughputs for multiple samples in these

* To whom correspondence should be addressed. E-mail: fangqun@zju.edu.cn.
† Present address: Department of Chemistry, University of Chicago, Chicago, IL 60637, United States.

(1) Song, H.; Chen, D. L.; Ismagilov, R. F. *Angew. Chem., Int. Ed.* **2006**, *45*, 7336–7356.
(2) Teh, S. Y.; Lin, R.; Hung, L. H.; Lee, A. P. *Lab Chip* **2008**, *8*, 198–220.
(3) Chiu, D. T.; Lorenz, R. M.; Jeffries, G. D. M. *Anal. Chem.* **2009**, *81*, 5111–5118.
(4) Taly, V.; Kelly, B. T.; Griffiths, A. D. *ChemBioChem* **2007**, *8*, 263–272.
(5) Song, H.; Tice, J. D.; Ismagilov, R. F. *Angew. Chem., Int. Ed.* **2003**, *42*, 767–772.
(6) Tan, Y. C.; Fisher, J. S.; Lee, A. I.; Cristini, V.; Lee, A. P. *Lab Chip* **2004**, *4*, 292–298.
(7) Ahn, K.; Kerbage, C.; Hunt, T. P.; Westervelt, R. M.; Link, D. R.; Weitz, D. A. *Appl. Phys. Lett.* **2006**, *88*, 024104.
(8) Chen, D. L.; Du, W. B.; Liu, Y.; Liu, W. S.; Kuznetsov, A.; Mendez, F. E.; Philipson, L. H.; Ismagilov, R. F. *Proc. Natl. Acad. Sci. U.S.A.* **2008**, *105*, 16843–16848.
(9) Zheng, B.; Ismagilov, R. F. *Angew. Chem., Int. Ed.* **2005**, *44*, 2520–2523.
(10) He, M. Y.; Edgar, J. S.; Jeffries, G. D. M.; Lorenz, R. M.; Shelby, J. P.; Chiu, D. T. *Anal. Chem.* **2005**, *77*, 1539–1544.
(11) Wei, C. W.; Cheng, J. Y.; Huang, C. T.; Yen, M. H.; Young, T. H. *Nucleic Acids Res.* **2005**, *33*, e78.
(12) Han, Z. Y.; Li, W. T.; Huang, Y. Y.; Zheng, B. *Anal. Chem.* **2009**, *81*, 5840–5845.
(13) Frenz, L.; El Harrak, A.; Pauly, M.; Bégin-Colin, S.; Griffiths, A. D.; Baret, J. C. *Angew. Chem., Int. Ed.* **2008**, *47*, 6817–6820.
(14) Thorsen, T.; Roberts, R. W.; Arnold, F. H.; Quake, S. R. *Phys. Rev. Lett.* **2001**, *86*, 4163–4166.
(15) Anna, S. L.; Bontoux, N.; Stone, H. A. *Appl. Phys. Lett.* **2003**, *82*, 364–366.

10.1021/ac1020479
Published on Web 11/02/2010

systems are limited by the world-to-chip interface problem.[16] To screen multiple targets without the limitation described above, the cartridges consisting of a sequentially aspirated droplet array stored in a tubing[9,17] (Figure 1c) were adopted to introduce different target droplets into the screening systems. This technique was applied in protein crystallization screening by first manually generating submicroliter plugs containing different precipitants in a cartridge and then making the cartridge plugs merge with protein stream in a T-junction channel to form mixed plugs (Figure 1e).[9] This technique was further improved using air spacing between different reagents in the cartridge to screen both different reagents and mixing ratios and employing air bubbles and droplet size to address the conditions.[18] In addition to the cartridge technique, an automated two-component droplet-based screening platform was also developed to perform sequential sampling, reagent mixing by droplet fusion (Figure 1d), and polymerase chain reaction in microliter-sized droplets.[19] In spite of the great success of the above-mentioned droplet-based microfluidic systems, the automated and rapid sample changing as well as the flexible and accurate control of the volume and composition of droplets in the picoliter to nanoliter range still present challenges.

Herein, we developed a droplet-based microfluidic system which we call "DropLab", using picoliter-scale liquid metering, sequential droplet assembling, and automated sample introduction techniques[20−24] to generate droplet arrays for multiple screening purposes with high controllability on the size and composition of each droplet. The system is also capable of performing parallel screening in linear or two-dimensional droplet arrays with extremely low sample and reagent consumptions. A novel droplet generation approach based on the droplet assembling strategy was used to produce multicomponent droplets in the nanoliter to picoliter range on demand. Such a strategy is different from those microfluidic devices utilizing the oil−aqueous interface instability to form droplets, in which multiple factors affect droplet size, such as liquid viscosity, channel geometry, and capillary number.[14,15] We demonstrated the versatility of DropLab in multiple applications including enzyme inhibition assay, protein crystallization screening, and identification of trace reducible carbohydrates.

EXPERIMENTAL SECTION

Chemicals and Materials. All solvents and chemicals used were of reagent grade unless otherwise stated. Deionized water was used throughout. *n*-Heptane, *n*-tetradecane, lysozyme from chicken egg white, and β-galactosidase from *Escherichia coli* (β-gal, 248 units/mg) were obtained from Sigma-Aldrich (St. Louis, MO). Fluorescein digalactoside (FDG) was obtained from Molecular Probes (Eugene, OR). Diethylenetriaminepentaacetic acid (DTPA) was purchased from Nanxiang Reagents Co. (Shanghai, China). Crystal Screen reagent kit (HR2-110) was purchased from Hampton Research (Aliso Viejo, CA). Potassium sodium tartrate, galactose, maltose, glucose, fructose, sucrose, starch, and Span 80 were purchased from Sangon Biotechnology Co. (Shanghai, China). Octadecyl-trichlorosilane was purchased from Acros Organics (Morris Plains, NJ). Food dyes were purchased from Shanghai Dyestuffs Research Institute (Shanghai, China). Fused-silica capillaries with 75 μm i.d. (375 μm o.d.), 150 μm i.d. (375 μm o.d.), and 200 μm i.d. (320 μm o.d.) were purchased from Reafine Chromatography Co. (Yongnian, China). Gastight syringes (1700 series, 10 μL) and Microliter syringes (7000 series, 1 μL) were purchased from Hamilton (Reno, NV).

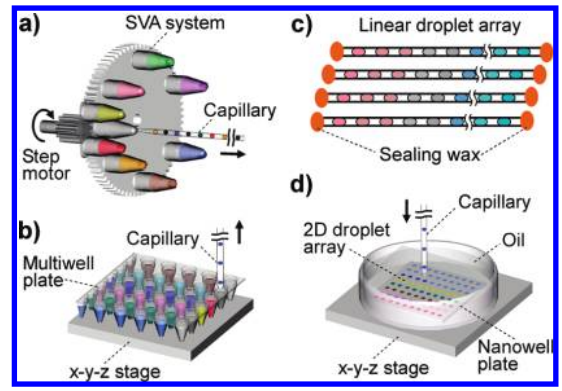

Figure 2. Setup of the DropLab system (not to scale). (a) DropLab with slotted-vial array. (b) DropLab with multiwell plate. (c) Droplet arrays sealed with wax for long-time storage. (d) 2D-droplet array formed by depositing the generated droplets in the capillary into an oil-immersed nanowell plate. The arrows represent the flow directions of liquids in the capillary channels.

Setup of the System. The DropLab system consists of three major components: a short capillary with a tapered tip for liquid metering and mixing, as well as droplet assembling and storing; a syringe pump (PHD2000, Harvard Apparatus, Holliston, MA) with picoliter precision connected with the capillary; an automated liquid presenting system based on either a slotted-vial array (SVA) fixed on gear plates (Figure 2a) or a 384-well plate for reagents, samples, and oil fixed on an *x-y-z* translation stage (Shanghai Lianyi Instrument Factory of Optical Fiber and Laser, Shanghai, China; Figure 2b). Both the automated liquid presenting systems and the syringe pump were under control of a program written in LabVIEW (National Instruments, Austin, TX). A stereoscopic microscope (SZM45, Sunny Optical Technology, Ningbo, China) and a CCD camera (G300UMD, HangZhou Glory Technology, Hangzhou, China) were used to observe the droplet generation. An inverted microscope (ECLIPSE TE-2000-S, Nikon, Japan) coupled with a CCD camera (SPOT RT-SE6, Diagnostic Instruments, Sterling Heights, MI) was used to observe the protein crystals and measure the fluorescent intensities of droplets.

The tapered capillary was fabricated by heating a straight capillary and then stretching the capillary by pulling both ends of it with a constant force. The shape and size (Figure S1, Supporting Information) of the tapered tip capillary was characterized by imaging with the inverted microscope coupled with the CCD camera. The inner and outer surfaces of the tapered capillary

(16) Liu, J.; Hansen, C.; Quake, S. R. *Anal. Chem.* **2003**, *75*, 4718–4723.
(17) Linder, V.; Sia, S. K.; Whitesides, G. M. *Anal. Chem.* **2005**, *77*, 64–71.
(18) Li, L.; Mustafi, D.; Fu, Q.; Tereshko, V.; Chen, D. L.; Tice, J. D.; Ismagilov, R. F. *Proc. Natl. Acad. Sci. U.S.A.* **2006**, *103*, 19243–19248.
(19) Chabert, M.; Dorfman, K. D.; Cremoux, P.; Roeraade, J.; Viovy, J. L. *Anal. Chem.* **2006**, *78*, 7722–7728.
(20) Fang, Q.; Shi, X. T.; Du, W. B.; He, Q. H.; Shen, H.; Fang, Z. L. *Trends Anal. Chem.* **2008**, *27*, 521–532.
(21) Du, W. B.; Fang, Q.; He, Q. H.; Fang, Z. L. *Anal. Chem.* **2005**, *77*, 1330–1337.
(22) Du, W. B.; Fang, Q.; Fang, Z. L. *Anal. Chem.* **2006**, *78*, 6404–6410.
(23) Zhang, T.; Fang, Q.; Du, W. B.; Fu, J. L. *Anal. Chem.* **2009**, *81*, 3693–3698.
(24) Du, W. B.; Dong, L.; Fang, Q. In *Proceedings of MicroTAS 2007 Conference*; Viovy, J. L., Tabeling, P., Descroix, S., Malaquin, L., Eds.; Paris, France, 2007; Chemical and Biological Microsystems Society: San Diego, CA; Vol. 2, pp 943−945.

were silanized with 4 mM octadecyl-trichlorosilane in *n*-heptane for 4 h at 25 °C before the experiments.

The automated liquid presenting system with slotted-vial array (SVA) is similar to that described previously[20−22] with some modifications. Smaller vials were made from the wells cut from a 384-well plate (see Figure S2, Supporting Information). A narrower slot (0.5 mm wide) was fabricated on the bottom of each vial using a razor blade to cut and remove a 0.5 mm wide, 0.8 mm deep slice from the center of the vial bottom. The slotted vials were arranged on a pair of gears with one pinion gear and one big gear (Figure 2a). The gear pair design[22] was developed to reduce the number of duplicated vials loaded with same liquid. The nanowell plate for droplet storage was fabricated based on a glass plate with chromium and photoresist coating (Shaoguang Microelectronics Co., Changsha, China) using the standard photolithographic and wet etching techniques. The diameter and depth of each well in this plate was 400 μm and 150 μm, respectively. The surface of the nanowell plate was silanized with 4 mM octadecyl-trichlorosilane in *n*-heptane for 4 h at 25 °C before the experiments.

Procedure. A 6 cm long, 150 μm i.d. capillary with a 25 μm i.d. at the tapered tip end was typically used unless mentioned otherwise. The other end of the capillary was connected with a 10 μL syringe equipped in the syringe pump. To use DropLab with the SVA system, the slotted vials were loaded with 5−10 μL of aqueous sample, reagent solutions, and oil. Droplet assembling was performed by rotating the array of vials, allowing the capillary tip to sequentially enter the liquids filled in the different vials through the slots, aspirating certain volumes of sample, reagents, and oil into the capillary with the syringe pump according to the program, respectively. For DropLab using the 384-well plate, the samples, reagents, and oil were loaded into different wells in the 384-well plate. Droplet assembling was performed by moving the *x-y-z* stage to allow the capillary tip to sequentially insert into the sample, reagent, and oil wells and aspirate programmed volumes of corresponding liquids into the capillary, which is similar to the operation described above for the SVA system.

Enzyme Inhibition Assay. An enzyme inhibition assay was performed using DropLab with the SVA system (Figure 2a). In the assay, 0.1 mg/mL β-galactosidase in 0.1 mM $MgCl_2$ and 10 mM Tris buffer at pH 7.3, 100 μM FDG in dimethylsulfoxide (DMSO), and DTPA were used as enzyme, substrate, and inhibitor, respectively. *n*-Tetradecane was used as carrier oil.

Protein Crystallization Screening. Protein crystallization screening was performed using DropLab with the 384-well plate and *x-y-z* translation stage (Figure 2b). A protein solution of 100 mg/mL lysozyme was prepared by dissolving 10 mg of lysozyme in 100 μL of 0.1 M NaAc buffer (pH = 4.6). Fifty precipitants (Table S1, Supporting Information), including 1.0 M NaCl and 25% polyethylene glycol (PEG) 6000 in 0.1 M NaAc buffer (pH = 4.6), and 49 precipitants in the Crystal Screen reagent kit (HR2-110, Hampton Research, Laguna Niguel, CA) were prepared fresh before use. The 50 precipitant solutions, lysozyme solution (100 mg/mL), and oil (tetradecane with 2% Span-80) were loaded into the corresponding wells on the 384-well plate. A 10 cm long capillary with 200 μm i.d and 60 μm tip i.d. was connected with a 10 μL syringe fixed on the syringe pump with a setting resolution of 300 pL.

Identification of Reducible Carbohydrates. Experiments for identification of reducible carbohydrates were performed using DropLab with the 384-well plate and the nanowell plate fixed on the same *x-y-z* translation stage. Six carbohydrate solutions of 0.1 mM galactose, 0.1 mM maltose, 0.1 mM glucose, 0.1 mM fructose, 0.1 mM sucrose, and 0.2 g/L starch were prepared by dissolving appropriate amounts of carbohydrates in water. Before the experiment, Fehling's solution was prepared by mixing equal volumes of Fehling's solution A [3.5% (w/v) $Cu_2SO_4 \cdot 5H_2O$] and Fehling's solution B [17% (w/v) potassium sodium tartrate tetrahydrate in 5% (w/v) NaOH]. *n*-Tetradecane was used as the carrier oil for droplet generation, as well as the oil covering the 2-D droplet array deposited from the capillary onto the nanowell plate.

RESULTS AND DISCUSSION

Building of the DropLab System. One of the main objectives of DropLab is to automatically assemble droplets in the nanoliter to picoliter range with high precision and flexibility from multiple samples and reagents stored in a convenient library platform. The DropLab system was built based on three components including a tapered capillary, a syringe pump connected to the capillary, and an automated liquid presenting system, without the need of microchips and microfabrication equipment. The capillary with a silanized tapered tip was used to decrease the tip surface area contacting with liquid when it inserted into the liquid for sampling and, thus, to reduce the cross-contamination between different droplets in the array. The use of the tapered capillary with tip inner diameter of 25−30 μm also ensures the implementation of picoliter-scale liquid metering and aspirating by coupling with the picoliter precision syringe pump. For the liquid presenting, we developed two systems based on the slotted-vial array (SVA)[20−24] technique and multiwell plates coupled with an *x-y-z* translation stage (Figure 2b), respectively.

The SVA technique is efficient and versatile for automated high-throughput sample introduction in continuous-phase microfluidic systems, such as microfluidic flow injection analysis (FIA),[21] sequential injection analysis (SIA),[22] and high-speed capillary electrophoresis.[23] In this work, we used it for the first time to assemble droplets for its capability of ultrafast liquids switching. The preliminary results were reported at a conference.[24] Since then, the system has been fully characterized with its functions and applications extended. For screening a large number of targets, we developed the robotic system compatible with 384-well plate. A nanowell plate fixed on the same *x-y-z* stage was also used to store the two-dimensional droplet array deposited from the capillary and facilitate the subsequent incubation and detection (Figure 2d).

The implementation of DropLab relies on four general steps: (i) load the robotic liquid presenting system with samples, reagents, and oil and input parameters of the droplet array into the program; (ii) run the program to sequentially aspirate certain volumes of sample, reagents, and oil into the capillary by the syringe pump to assemble a composite droplet (Figure 3a); (iii) assemble as many droplets as the program to form a droplet array which is either stored in the capillary (Figure 2c) or deposited into the oil-immersed nanowell plate (Figure 2d); (iv) perform parallel incubation, reaction, and assay in the droplet array.

To program an array consisting of n droplets, we define the droplet array with its sequence i and volume V, $V = \{V_1, V_2, \ldots V_i \ldots V_n\}$. For each composite droplet, it is assembled

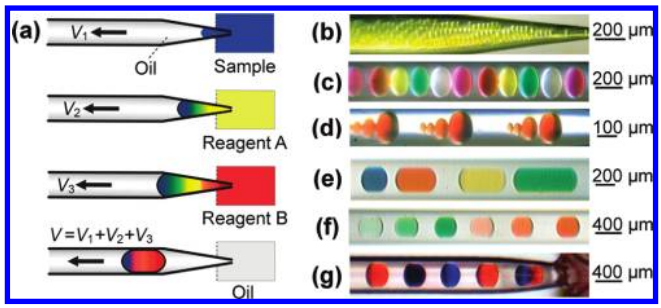

Figure 3. Principle and performance of DropLab. (a) Schematic diagram of principle for assembling a 3-component droplet using DropLab. (b) Continuous generation of 20 pL droplets with a throughput of 4.5 s per droplet by sequentially aspirating a 20 pL fluorescence solution and 80 pL of oil at flow rates of 2 and 8 nL/min, respectively. (c) Continuous generation of 1.6 nL droplets containing five different dyes. (d) Droplets with different volumes of 20, 40, 160, and 1000 pL generated with 0.6 s sampling time and increasing flow rates from 2 to 100 nL/min. (e) Droplets with different volumes (2.5, 4.5, 5.5, and 8.0 nL) and different dyes. (f) Series of 2.5 nL droplets with concentration gradient formed by diluting the green and red dye solutions with volume ratios of 1: 19, 1: 4, and 19: 1 (dye/water). (g) 2.5 nL droplets formed by sequentially introducing red dye, water, and blue dye with different mixing ratios of 1.0:1.5:0, 0.5:1.5:0.5, and 0:1.5:1.0.

by m different liquids, the total volume of the droplet is $V_i = \Sigma V_j t_j$ ($j = 1, 2, ...m$). Here, v_j is the aspiration flow-rate and t_j is the aspiration time for liquid j, both of which are programmed and controlled by the syringe pump. The volume percentage of each liquid in the droplet could be calculated with $P_{ij} = V_j t_j / V_i$. Thus, the exact concentration of each component in every droplet could be expressed by $C_{ij} = C_j P_{ij}$, where C_j is the original concentration of component in liquid j. This assembling strategy for array of multiple component droplets is flexible in droplet size, composition, and sequence (Figure 3a).

System Performance. We first demonstrated the performance of DropLab in droplet generation with the SVA system using food dye solutions and tetradecane oil as the dispersed and continuous phases. Benefiting from the use of the tapered-tip capillary and the picoliter-scale precision syringe pump with a 1 μL syringe, the minimum unit of the droplet volume in the present system reached ~20 pL. At a speed of 4.5 s per droplet, 400 droplets of 20 pL were aspirated in a 30 min experiment (Figure 3b). With this capability, the volume ratio between the liquids introduced into a droplet could reach 1:400 on demand, which significantly improved the control ability of DropLab in the droplet compositions. Various nanoliter-scale composite droplets with different size, composition, and sequence were readily assembled by adjusting the type, volumes, and mixing ratios of aspirated liquids (Figure 3c–g). In Figure 3c, an array of 100, 1.6 nL droplets aspirated from five slotted vials containing different dye solutions was sequentially generated with a throughput of ~9 s per droplet. In Figure 3d, an array of 4 droplets with volumes of 20, 80, 200 and 1000 pL were generated within 48 s. Repeatedly, 18 duplicates of such arrays (totally 72 droplets) were generated in 15 min. Droplets with different volumes (2.5, 4.5, 5.5, and 8.0 nL) and different dyes were generated in a sequence as shown in Figure 3e. In Figure 3f, a series of 2.5 nL two-component (dye solution and water) droplets with concentration gradients were formed by diluting the green or red dye solutions with water. In Figure 3g, a series of 2.5 nL three-component droplets was formed by sequentially introducing red dye, water, and blue dye with different mixing ratios. The aspirating flow rates in Figure 3e–g were controlled at 60–100 nL/min, and droplets were generated continuously with average throughputs of ca. 10 s per droplet.

As DropLab is actively controlled by computer programs, its droplet generation throughputs are typically around 5–15 s per droplet, depending on droplet size and composition. These are slower than those passive droplet formation methods[2] based on microfluidic networks which are able to generate droplets with frequencies from 2 to 5300 Hz. However, DropLab is designed to automatically and flexibly generate droplet arrays aiming to multiple screening purposes. Without the need of microfabricated devices, tens to hundreds of droplet-based experiments could be performed in a short capillary of DropLab.

The droplet storing capacity for a capillary is dependent upon the volumes of droplets and oil spaces, as well as the capillary length and inner diameter. Typically, 100–200, 2 nL droplets could be generated and stored in a 6 cm long, 150 μm i.d. capillary. Increasing the capillary length could increase the droplet storing capacity of the capillary. However, this was limited by the increase of flow resistance in the capillary channel which affected the liquid aspirating precision. For storing a larger number of droplets, multiple capillaries could be employed (see Protein Crystallization Screening).

In DropLab, the use of the tapered capillary tip with a silanized outer surface also effectively reduced the cross-contamination between different liquids. We evaluated the carryover between two adjacent droplets by alternatively aspirating 2 nL, 100 μM fluorescein and water droplets. Compared with the plane-tip capillary, the carryover of the tapered-tip capillary was significantly reduced from 6% to 0.4%. This carryover could be further reduced to 0.01% by placing a tip-washing water vial between the adjacent sample vials with a tip residence time of 2 s in this vial.

We further tested the precision and reproducibility of DropLab in assembling nanoliter droplets by diluting 1 mM fluorescein using buffer with a different dilution percentage. A series of 10 nL droplets was assembled with 0.2%, 0.5%, 1%, 5%, 10%, 25%, 50%, and 75% dilutions of the fluorescein solution using a 6 cm long capillary with 200 μm i.d. and 20 μm tip i.d. The same 1 mM fluorescein solution was diluted offline using standard pipetting method to produce the calibration curve. A good linear relationship ($r^2 = 0.9989$) between the theoretical dilution concentrations and the actual measured concentrations of fluorescein in the droplets was obtained (Figure 4). The droplet array was reproduced, and the relative standard deviation (RSD) for a 50% dilution was 3.6% ($n = 5$).

Enzyme Inhibition Assay. We applied the DropLab system in enzyme inhibition assay to demonstrate its potential feasibility in low-consumption drug screening. The assay was based on the inhibition of β-galactosidase by inhibitor (diethylenetriaminepentaacetic acid, DTPA) solutions with different concentrations, impeding the conversion of substrate FDG to fluorescein. A series of 2 nL droplet reactors with the same enzyme and substrate concentrations and different inhibitor concentrations were assembled with DropLab at a throughput of 4.5 s per droplet. The fluorescence intensities of the droplets were measured after a 10

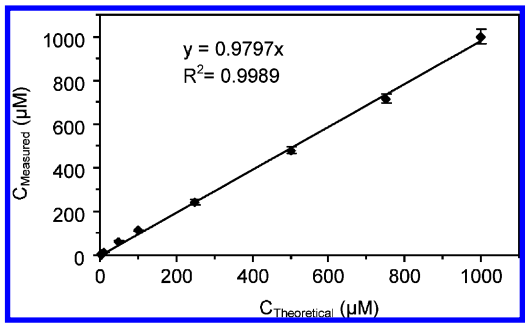

Figure 4. Linear regression curve of the theoretical dilution concentrations and the actual measured concentrations of fluorescein in the 10 nL droplets generated with DropLab. The error bars are the standard deviation obtained from five droplets.

min reaction time with the fluorescence microscope and CCD camera (Figure 5a). An inhibition curve in the range of 0−5.0 mM DTPA was obtained by defining the intensity of 0 mM DTPA to be 100% (i.e., 0% inhibition; Figure 5c). The half maximal inhibitory concentration (IC50) deduced from this curve was 0.7 mM DTPA, which is similar to the result reported previously.[25] In DropLab, each droplet had different compositions, aimed at individual screening measurements. Therefore, the sample and reagent consumptions for each measurement could be significantly reduced from the microliter or nanoliter range to several hundred picoliters. Only four 2 nL droplets containing enzyme, substrate, and inhibitor with different concentrations of 0, 0.5, 1.0, and 5.0 mM were required to obtain the inhibition curve and the IC50 value for an inhibitor. This feature is advantageous for reducing screening cost and, thus, particularly valuable for screening with rare and expensive samples and reagents, such as drug screening.

Protein Crystallization Screening. The DropLab system was also applied in automated screening and optimization of crystallization conditions for a model protein lysozyme. Fifty precipitants with different concentrations of salts, precipitants, and buffers at different pH values were chosen to perform the screening. A series of 50, 12 nL droplets composed of 6 nL of protein solution and 6 nL of different precipitants was generated in a 10 cm long capillary within 22.5 min as the sequence shown in Figure 6a. The length of the droplet array in the capillary with 20 nL oil spaces between the droplets was 6 cm. This throughput of droplet generation was relatively lower than those in performance experiments due to the longer aspirating time and lower aspirating flow rate which were chosen to match the high viscosity of the protein and precipitant solutions. To eliminate the effects of the crystallization condition fluctuation, and the droplet size variation due to the high viscosities of protein and precipitant solutions, parallel experiments were performed by sequentially generating eight linear droplet arrays (totally 400 droplets) in eight capillaries in 3.2 h (see Figure S3, Supporting Information). These capillaries were sealed with wax and incubated for crystallization at 20 °C. Figure 6b shows typical images of 50 droplets in the droplet array of one capillary after a 20 h incubation. Eight parallel experiments showed similar results that lysozyme crystals were observed in the droplet with precipitant #1 of 1.0 M NaCl and 25% PEG 6000 in 0.1 M NaAc buffer (pH = 4.6; Figure 6b,c). No crystal was observed in other precipitant condition droplets even after a 36 h incubation period. To optimize the lysozyme crystal growth with precipitant #1, we aspirated the protein and precipitant solutions with different mixing ratios of 4:1, 2:1, 1:1, 1:2, and 1:4. For each mixing ratio, two copies of droplets were generated in a 10 droplet sequence. Totally, 40 droplets were generated in one capillary with 4 duplicates (Figure 6d). The screening results are shown in Figure 6e. Similar crystal growth results were observed in all four duplicates. On the basis of the analysis of the number, shape, and size of the crystals, the optimal crystallization condition was obtained with a 1:2 mixing ratio for lysomze and precipitant #1.

Identification of Reducible Carbohydrates. The performance of the DropLab with the nanowell plate was further demonstrated in the identification of trace amounts (0.2−2.5 ng) of reducible carbohydrates (Figure 7). In this assay, the reduction reaction of carbohydrate and Fehling's solution should be conducted at 100 °C; thus, the capillary-based droplet storage method was not feasible due to the liquid expansion and boiling by heating. Equal volumes of carbohydrate solution and Fehling's solution were sequentially aspirated into the capillary from the 384 well plate to assemble a 25 nL droplet; then, the droplet was deposited onto the oil-immersed nanowell plate. The nanowell plate was placed on a 110 °C heater for a 5 min reaction. The carbohydrates with aldehyde or carbonyl group, i.e., glucose, fructose, maltose,

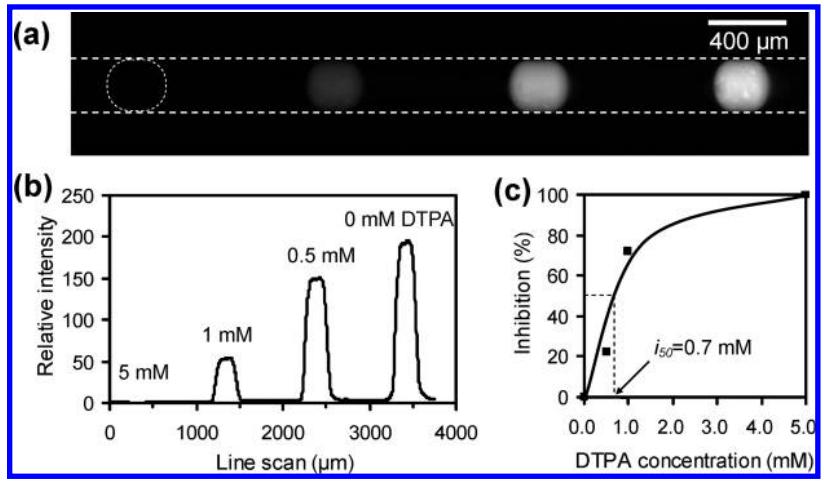

Figure 5. Profiling inhibition of enzyme catalyzed reaction using DropLab. (a) Fluorescent microphotograph of a series of 2 nL droplet reactors containing enzyme (β-galactosidase), substrate (FDG), and inhibitor (DTPA) with different DTPA concentrations of 0, 0.5, 1.0, and 5.0 mM. (b) Relative fluorescence intensities in each droplet shown in (a). (c) Inhibition curve obtained from (b).

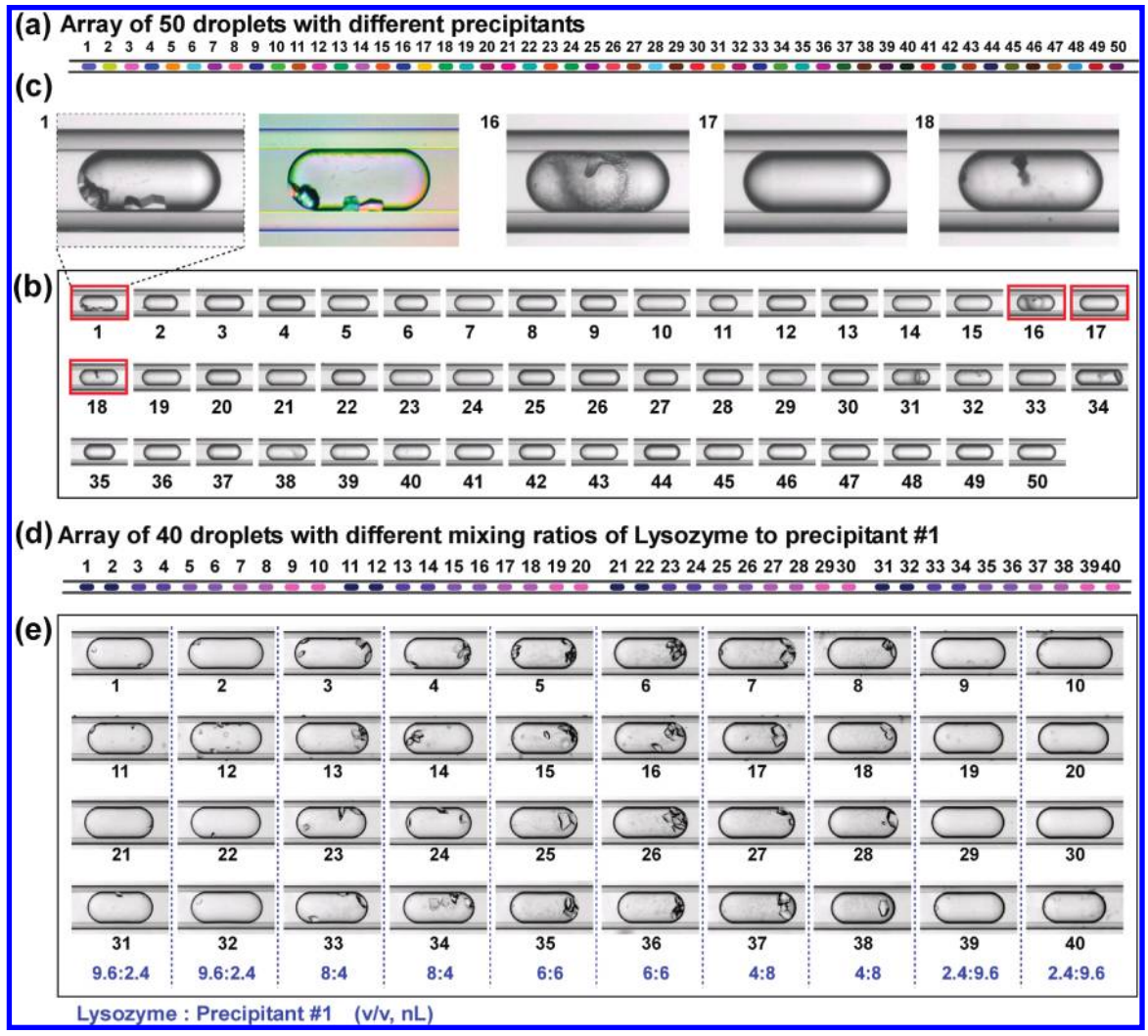

Figure 6. Protein crystallization screening and optimization using DropLab. (a) Schematic diagram of the droplet array for screening of 50 different precipitants in a capillary. (b) Typical images of 50 droplets containing protein lysozyme and 50 different precipitants in the droplet array of one capillary after a 20 h incubation. Aspirating flow rate, 200 nL/min; droplet volume, 12 nL; oil space between droplets, 20 nL. (c) Enlarged views of droplets containing precipitant #1, #16, #17, and #18 in (b). Evident lysozyme crystals were observed in droplet #1. The second image of droplet #1 is a polarized microphotograph illustrating the lysozyme crystals. (d) Schematic diagram of droplet array for optimization of mixing ratio of protein to precipitant #1 in a capillary. (e) Individual images of 40 droplets (4 duplicates) in the screening array with different mixing ratios of 4:1, 2:1, 1:1, 1:2, and 1:4 between lysozyme and precipitant #1. Droplet volume: 12 nL; oil space between droplets, 15 nL. In each column of (e), the droplets have the same mixing ratio as listed at the bottom of the column.

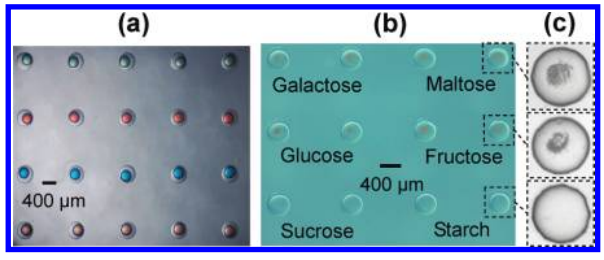

Figure 7. (a) Image of 2-D array of 12 nL droplets containing different dyes automatically produced by depositing the assembled droplets in the capillary onto the nanowell plate. (b) Identification of reducible carbohydrates in a 25 nL droplet array using the reaction of carbohydrates and Fehling reagent. Precipitates of Cu_2O were produced in droplets containing reducible carbohydrates. (c) Enlarged views of nanowells in (b).

and galactose, reacted with Fehling reagent and produced a precipitate of Cu_2O in droplets, while the droplets containing sucrose or starch without reactive groups were clear. Compared with the linear droplet array stored in a capillary, the capacity of the 2D droplet array has a quadratic increase. Another advantage of the oil-immersed 2D droplet array is that it converts the droplet array from a close system to an open system, which would significantly facilitate the addition of new reagents to droplets and extraction of specific droplet for further detection.

CONCLUSION

In summary, we have established DropLab, an automated, flexible, and versatile platform for performing chemical and biological reactions and screenings in a nanoliter-scale droplet array. The broad applicability of DropLab was demonstrated in multiple applications of enzyme inhibition assay, protein crystallization screening, and identification of reducible carbohydrates. DropLab does not rely on complex microchannel networks and shows significant improvements in control scope and precision

(25) Pu, Q. S.; Liu, S. R. *Anal. Chim. Acta* **2004**, *511*, 105–112.

for the liquid metering and mixing and, thus, for the volumes and compositions of the assembled droplets. Compared with the commercial or reported robotic liquid handling systems[26,27] for automated screening with microliter or nanoliter precision, DropLab has picoliter precision and the smallest droplet sizes to several hundred picoliters, which can reduce sample and reagent consumptions by 1−4 orders of magnitude. These characteristics are likely to meet the increasing demands on automatic liquid handling for low consumption and large-scale screening. Although the throughput of droplet generation in DropLab is relatively lower than those in droplet systems based on passive continuous flow mode, the aim of DropLab is not to compete with the existing microfluidic devices on number and speed of droplet generation but to improve the diversity of droplets and the number of screening conditions with extremely low consumptions. Moreover, the throughput of DropLab could be further improved using a multicapillary array.

We believe that DropLab could find broad applications in drug discovery, clinical diagnosis, reaction screening, and cell-based assays. With the advance of automated droplet imaging and detection techniques, it is possible to upgrade the DropLab system to an intelligent platform for programmable scientific research.[28]

ACKNOWLEDGMENT

W.-B.D., M.S., S.-Q.G., and Y.Z. contributed equally to this work. Financial support from National Natural Science Foundation of China (Grants 0775071, 20825517,and 20890020), Ministry of Science and Technology of China (Grants2007CB714503 and 2007CB914100), and the Fundamental Research Funds for the Central Universities of China are gratefully acknowledged.

SUPPORTING INFORMATION AVAILABLE

Additional information as noted in text. This material is available free of charge via the Internet at http://pubs.acs.org.

Received for review August 2, 2010. Accepted October 20, 2010.

AC1020479

(26) Jenkins, J.; Cook, M. *JALA* **2004**, *9*, 257–261.
(27) Wang, J. B.; Zhou, Y.; Qiu, H. W.; Huang, H.; Sun, C. H.; Xi, J. Z.; Huang, Y. Y. *Lab Chip* **2009**, *9*, 1831–1835.
(28) King, R. D.; Rowland, J.; Oliver, S. G.; Young, M.; Aubrey, W.; Byrne, E.; Liakata, M.; Markham, M.; Pir, P.; Soldatova, L. N.; Sparkes, A.; Whelan, K. E.; Clare, A. *Science* **2009**, *324*, 85–89.

SUPPORTING INFORMATION FOR

Automated Microfluidic Screening Assay Platform Based on DropLab

*Wen-Bin Du†, Meng Sun, Shu-Qing Gu, Ying Zhu and Qun Fang**

Institute of Microanalytical Systems, Department of Chemistry, Zhejiang University, Hangzhou 310058, China

The first four authors contributed equally to this work.

* To whom correspondence should be addressed. E-mail: fangqun@zju.edu.cn

†Present address: Department of Chemistry, University of Chicago, Chicago, IL 60637, USA

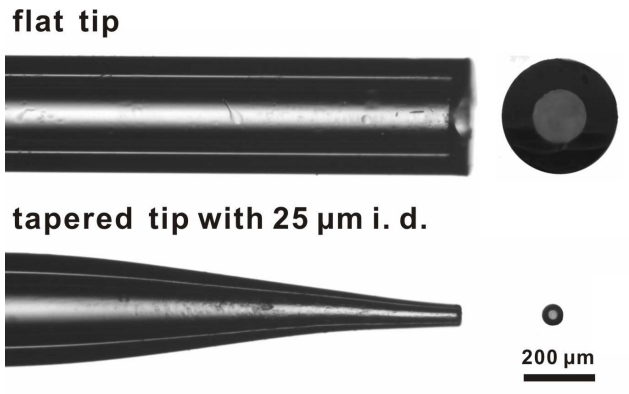

Figure S1. Images of a flat tip capillary (150 μm i.d) and a tapered fused silica capillary (inner diameter of tip end, 25 μm). Left: viewing from side; Right: viewing from the cross section of the tip end.

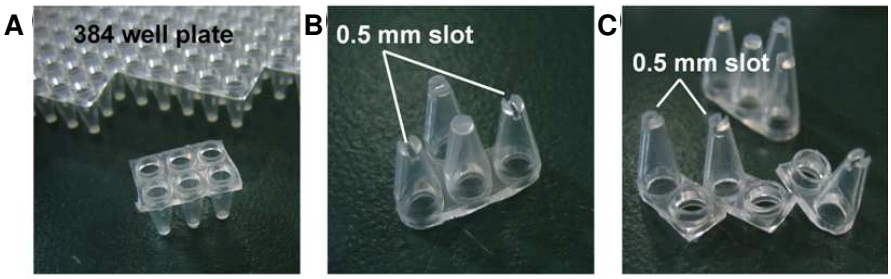

Figure S2. Fabrication of slotted vial arrays. (A) 30 μL vials cut from 384-well plate. (B) and (C) Slotted vials with 0.5-mm-wide slots fabricated on the bottom of each vial.

Figure S3. Image of eight 10-cm-long capillaries in parallel experiments for lysozyme crystallization screening. Each capillary stored 50 droplets for screening of 50 precipitants as listed in Table S1.

Table S1. Compositions of the screened protein precipitants.

	Salt	Buffer	Precipitants
1	1.0 M Sodium chloride	0.1 M Sodium acetate trihydrate pH 4.6	25% w/v Polyethylene glycol 6,000
2	0.02 M Calcium chloride dihydrate	0.1 M Sodium acetate trihydrate pH 4.6	30% v/v (+/-)-2-Methyl-2,4-pentanediol
3	None	None	0.4 M Potassium sodium tartrate tetrahydrate
4	None	None	0.4 M Ammonium phosphate monobasic
5	None	0.1 M TRIS hydrochloride pH 8.5	2.0 M Ammonium sulfate
6	0.2 M Sodium citrate tribasic dihydrate	0.1 M HEPES sodium pH 7.5	30% v/v (+/-)-2-Methyl-2,4-pentanediol
7	0.2 M Magnesium chloride hexahydrate	0.1 M TRIS hydrochloride pH 8.5	30% w/v Polyethylene glycol 4,000
8	None	0.1 M Sodium cacodylate trihydrate pH 6.5	1.4 M Sodium acetate trihydrate
9	0.2 M Sodium citrate tribasic dihydrate	0.1 M Sodium cacodylate trihydrate pH 6.5	30% v/v 2-Propanol
10	0.2 M Ammonium acetate	0.1 M Sodium citrate tribasic dihydrate pH 5.6	30% w/v Polyethylene glycol 4,000
11	0.2 M Ammonium acetate	0.1 M Sodium acetate trihydrate pH 4.6	30% w/v Polyethylene glycol 4,000
12	None	0.1 M Sodium citrate tribasic dihydrate pH 5.6	1.0 M Ammonium phosphate monobasic
13	0.2 M Magnesium chloride hexahydrate	0.1 M HEPES sodium pH 7.5	30% v/v 2-Propanol
14	0.2 M Sodium citrate tribasic dihydrate	0.1 M TRIS hydrochloride pH 8.5	30% v/v Polyethylene glycol 400
15	0.2 M Calcium chloride dihydrate	0.1 M HEPES sodium pH 7.5	28% v/v Polyethylene glycol 400
16	0.2 M Ammonium sulfate	0.1 M Sodium cacodylate trihydrate pH 6.5	30% w/v Polyethylene glycol 8,000
17	None	0.1 M HEPES sodium pH 7.5	1.5 M Lithium sulfate monohydrate
18	0.2 M Lithium sulfate monohydrate	0.1 M TRIS hydrochloride pH 8.5	30% w/v Polyethylene glycol 4,000
19	0.2 M Magnesium acetate tetrahydrate	0.1 M Sodium cacodylate trihydrate pH 6.5	20% w/v Polyethylene glycol 8,000
20	0.2 M Ammonium acetate	0.1 M TRIS hydrochloride pH 8.5	30% v/v 2-Propanol

21	0.2 M Ammonium sulfate	0.1 M Sodium acetate trihydrate pH 4.6	25% w/v Polyethylene glycol 4,000
22	0.2 M Magnesium acetate tetrahydrate	0.1 M Sodium cacodylate trihydrate pH 6.5	30% v/v (+/-)-2-Methyl-2,4-pentanediol
23	0.2 M Sodium acetate trihydrate	0.1 M TRIS hydrochloride pH 8.5	30% w/v Polyethylene glycol 4,000
24	0.2 M Magnesium chloride hexahydrate	0.1 M HEPES sodium pH 7.5	30% v/v Polyethylene glycol 400
25	0.2 M Calcium chloride dihydrate	0.1 M Sodium acetate trihydrate pH 4.6	20% v/v 2-Propanol
26	None	0.1 M Imidazole pH 6.5	1.0 M Sodium acetate trihydrate
27	0.2 M Ammonium acetate	0.1 M Sodium citrate tribasic dihydrate pH 5.6	30% v/v (+/-)-2-Methyl-2,4-pentanediol
28	0.2 M Sodium citrate tribasic dihydrate	0.1 M HEPES sodium pH 7.5	20% v/v 2-Propanol
29	0.2 M Sodium acetate trihydrate	0.1 M Sodium cacodylate trihydrate pH 6.5	30% w/v Polyethylene glycol 8,000
30	None	0.1 M HEPES sodium pH 7.5	0.8 M Potassium sodium tartrate tetrahydrate
31	0.2 M Ammonium sulfate	None	30% w/v Polyethylene glycol 8,000
32	0.2 M Ammonium sulfate	None	30% w/v Polyethylene glycol 4,000
33	None	None	2.0 M Ammonium sulfate
34	None	None	4.0 M Sodium formate
35	None	0.1 M Sodium acetate trihydrate pH 4.6	2.0 M Sodium formate
36	None	0.1 M HEPES sodium pH 7.5	0.8 M Sodium phosphate monobasic monohydrate 0.8 M Potassium phosphate monobasic
37	None	0.1 M Sodium acetate trihydrate pH 4.6	8% w/v Polyethylene glycol 4,000
38	None	0.1 M HEPES sodium pH 7.5	1.4 M Sodium citrate tribasic dihydrate
39	None	0.1 M HEPES sodium pH 7.5	2% v/v Polyethylene glycol 400 2.0 M Ammonium sulfate
40	None	0.1 M Sodium citrate tribasic dihydrate pH 5.6	20% v/v 2-Propanol 20% w/v Polyethylene glycol 4,000
41	None	0.1 M HEPES sodium pH 7.5	10% v/v 2-Propanol

			20% w/v Polyethylene glycol 4,000
42	0.05 M Potassium phosphate monobasic	None	20% w/v Polyethylene glycol 8,000
43	None	None	30% w/v Polyethylene glycol 1,500
44	None	None	0.2 M Magnesium formate dihydrate
45	0.2 M Zinc acetate dihydrate	0.1 M Sodium cacodylate trihydrate pH 6.5	18% w/v Polyethylene glycol 8,000
46	0.2 M Calcium acetate hydrate	0.1 M Sodium cacodylate trihydrate pH 6.5	18% w/v Polyethylene glycol 8,000
47	None	0.1 M Sodium acetate trihydrate pH 4.6	2.0 M Ammonium sulfate
48	None	0.1 M TRIS hydrochloride pH 8.5	2.0 M Ammonium phosphate monobasic
49	1.0 M Lithium sulfate monohydrate	None	2% w/v Polyethylene glycol 8,000
50	0.5 M Lithium sulfate monohydrate	None	15% w/v Polyethylene glycol 8,000